ROYAL NORWEGIAN COUNCIL FOR SCIENTIFIC AND INDUSTRIAL RESEARCH

PROCEEDINGS FROM THE
SEMINAR ON

SEISMOLOGY AND SEISMIC ARRAYS

OSLO, 22–25 NOVEMBER 1971

Editors: E S Husebye and H Bungum

Arranged in connection with the opening of The Norwegian Seismic Array (NORSAR) 1972

SIMULATING ARRAY EVENT LOCATION CAPABILITIES

H. GJØYSTDAL, E.S. HUSEBYE AND D. RIEBER-MOHN

NTNF/NORSAR
Kjeller, Norway

INTRODUCTION

A new dimension to the location of seismic events is represented by the large aperture arrays like LASA and NORSAR. These stations both detect and locate many events which are left unreported by an organization like NOAA (previously USCGS). We have investigated the above problem emphasizing the estimate of 95% confidence ellipses for event locations based on data from one or two arrays. The latter restriction is introduced as the LASA and NORSAR arrays have a direct communication link for mutual data exchange. Moreover, we have chosen whenever possible a quite general approach to the above problem, i.e., a simulation on the computer of the array location process in terms of random and biased errors in the observational data like arrival time, azimuth and velocity of the incoming wavefront.

The purpose of this paper is to present a method for simulating the event location capabilities of one and two arrays. Finally, its usefulness is demonstrated utilizing NORSAR and LASA bulletin data.

ONE-ARRAY EPICENTER LOCATION

Routine processing of events detected by large aperture arrays like LASA and NORSAR comprises calculations of azimuth and apparent velocity of the incoming P-waves. The latter parameter is easily converted to epicentral distance using standard travel time tables. Considering the spherical triangle whose corners are the North Pole, the array center and the event location (see Fig 1a), we are now in a position to compute the latitude and longitude of the epicenter using the basic trigonometric equations for spherical triangles.

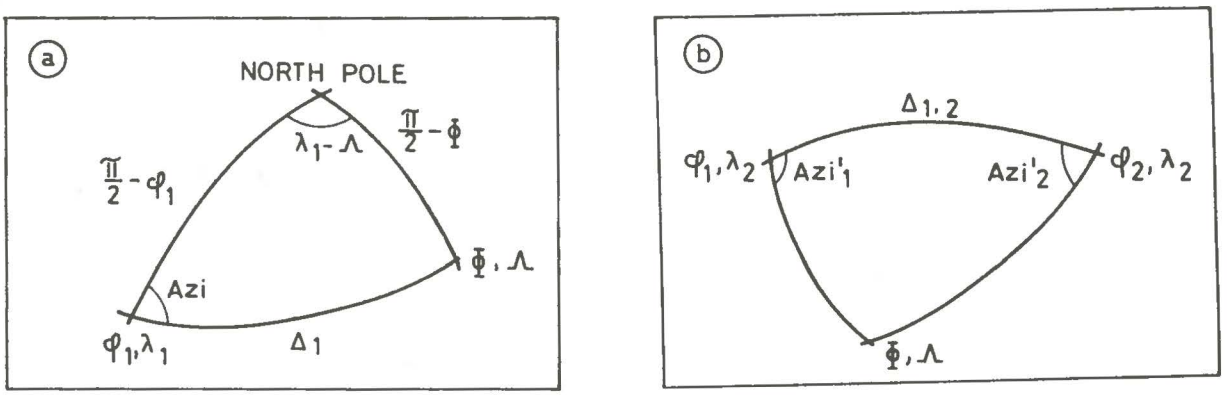

Fig 1. Principles for epicenter locations using one and two arrays. In each case at least two sides and angles are known in the given spherical triangles. Array and epicenter coordinates are denoted by (ϕ,λ) and (Φ,Λ) respectively. The indices 1 and 2 denote different arrays.

The next step is to obtain a random Gaussian distribution of the parameters azimuth and slowness (DT/DΔ). Specifying their mean values and variances 200 paired values of these two parameters are simulated by using a random number generation routine. These observations determine a distribution of event locations in geographic space, each point having a unique latitude and longitude. For computational convenience, we are pointing the array towards a specified point on the equator, i.e., o.o. N and o.o. E. In other words, when dealing with different epicentral distance intervals, the fictive array may be moved northwards in steps of say 10 deg as actually used. The simulated epicenters are considered in a Carthesian coordinate system, and the axes of the 95% confidence ellipse are computed using a method described by Evernden (1969).

In Table 1 the simulated one-array event location capability in terms of specified standard deviations of the DT/DΔ and azimuth parameters are tabulated. The calculated semi-axes of the 95% confidence ellipses are based on paired values, i.e., (σ(DT/DΔ) = 0.5 sec/deg, σ(Azi) = 1.0 deg), etc. However, as the above parameters are approximately independent of each other, confidence ellipses based on other σ(DT/DΔ), σ(Azi) combinations are obtainable from Table 1. This has been verified by several test runs.

EPI: DIST. (deg)	δ(DT/DΔ) IN SEC/DEG							δ|AZIMUTH| IN DEG						
	(1) 0.05	(2) 0.10	(3) 0.15	(4) 0.20	(5) 0.25	(6) 0.30	(7) 0.35	(1) 1.0	(2) 1.5	(3) 2.0	(4) 2.5	(5) 3.0	(6) 3.5	(7) 4.0
20	0.3	0.5	0.7	1.0	1.3	1.6	1.8	0.8	1.1	1.6	2.2	2.4	2.9	3.2
30	3.3	5.5	7.4	8.5	10.5	11.5	12.9	1.3	1.7	2.3	3.0	3.5	4.1	5.3
40	2.0	4.0	5.8	7.7	8.6	11.1	12.7	1.5	2.4	2.9	3.9	4.7	5.4	6.4
50	1.8	3.4	4.8	6.6	8.3	10.4	12.1	1.6	3.0	3.6	4.3	5.9	6.6	7.8
60	1.8	3.5	5.8	7.3	8.4	10.7	11.9	2.2	3.0	4.3	5.2	6.7	7.0	9.2
70	1.5	3.2	4.7	6.3	8.3	10.4	12.3	2.4	3.7	4.4	5.8	7.0	7.4	9.4
80	1.7	3.4	4.1	6.3	7.7	8.7	10.8	2.0	3.3	4.6	5.9	6.9	9.1	9.8
SEMI-AXES OF 95 % CONFIDENCE ELLIPSES IN DEG														

TABLE 1

Length in degrees of the semi-axes of the 95% confidence ellipses as a function of epicentral distances and standard deviations of observed slowness and azimuth. The given semi-axes are based on paired values of $\sigma(ST/D\Delta)$ and $\sigma(Azi)$ like $\Sigma_{11}, \Sigma_{22}, \ldots, \Sigma_{77}$ or (0.05, 1.0) etc.

EPICENTER LOCATION USING TWO ARRAYS

In this section the joint epicenter location capability of two arrays is simulated. The analysis is restricted to azimuth and arrival time differences, i.e., the slowness parameter is omitted. The reason is that in most cases the difference in arrival times gives a better distance estimate than that based on slowness measurements.

Given the observed azimuth at two different stations we can easily calculate the event position in geographic space as evident from Fig 1b. The simulation of the epicenter location process is quite similar to that one discussed in the previous section. As before, we can determine the point distribution in geographic space and then the probability surface which gives the axes and orientation of the 95% confidence ellipse.

When working with body waves it is logical to constrain the above arrival time differences. For a specific event location this parameter defines a curve in geographic space. We may assume that the associated probability density function is represented by a Gaussian surface along the curves of constant arrival time differences which may be considered to be parallel straight lines. Using the notations $f(x,y)$ and $g(x,y)$ for the azimuth and time difference probability distributions, it is possible to determine the epicenter or the point of maximum likelihood by forming the product

$$F(x,y) = f(x,y) \cdot g(x,y)$$

and then differentiating. The above method is described in detail in another paper by the authors (Gjøystdal et al, 1972).

The two-array epicenter location methods are demonstrated in Fig 2, using the data simulation approach outlined above. The procedure will be especially effective in case the confidence ellipse has a considerable eccentricity and the time difference line is nearly parallel to the shortest axis , e.g., when the two azimuth lines intersect under a very sharp angle.

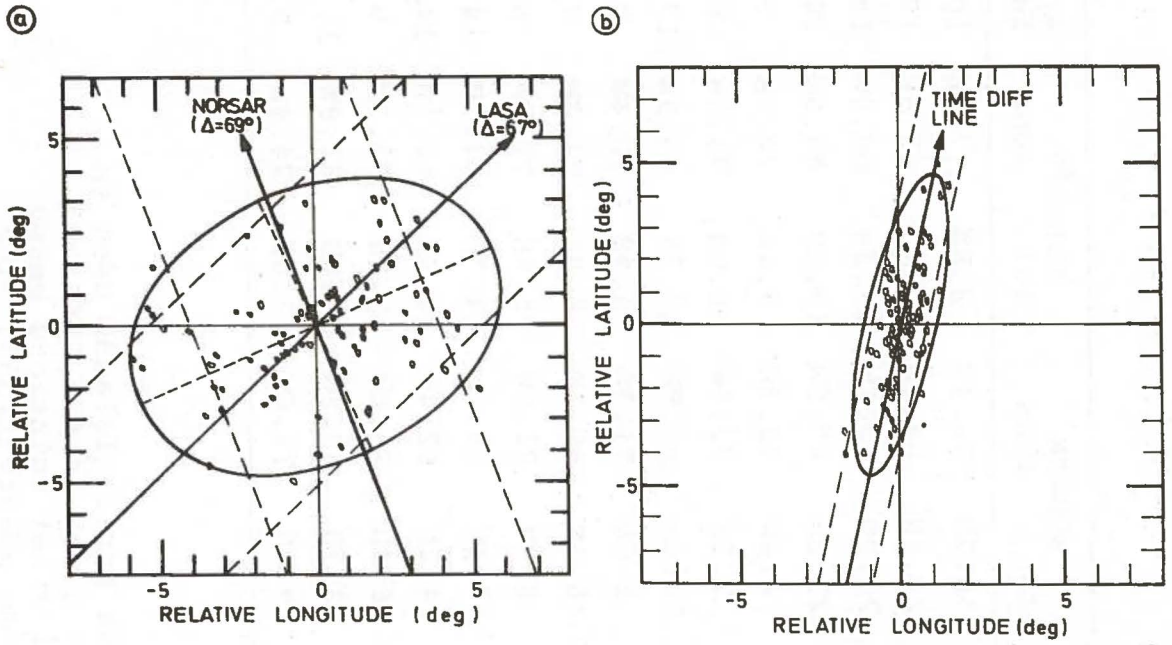

Fig 2. Simulated two-array event locations at 45.3°N, 149.3°E. The standard deviations of both azimuth observations are 2.0 deg, and those of arrival times 2.0 sec.

A small test of the joint location capabilities of the NORSAR and LASA arrays has been performed, using a number of the Kurile Islands events which are listed in Table 2. The results are displayed in Fig 3 and a few comments are as follows: Due to its larger aperture LASA is expected to have in general a better location performance than NORSAR and this is valid for the events analyzed. The preliminary location distribution vectors in use at NORSAR seem to be troubled by small systematic errors, and a bias correction of 1 deg in the azimuth estimate was introduced for the Kurile Islands event. Even better epicenter locations should be obtainable if absolute travel time corrections for the two arrays were available. Another factor of some importance is the shape of the azimuth confidence ellipse as the intersection between this and the line of constant time difference determines the final solution. Unfortunately, estimates of azimuth variances for LASA and NORSAR were not available.

NO.	DATE m/d/y	O.TIME h/m/s	T_N-T_L sec	MAG m_b	D km	NOAA lat	NOAA long	LASA lat	LASA long	NORSAR lat	NORSAR long	AZIMUTH lat	AZIMUTH long	AZI.&TIME lat	AZI.&TIME long
1	06/06/71	10/38/05	252.5	4.1	35	8.6N	79.3W	10N	78W	10.7N	76.1W	8.8N	77.3W	10.2N	78.2W
2	06/12/71	19/18/48	162.0	5.0	43	18.9N	64.3W	19N	65W	22.8N	63.4W	19.7N	65.6W	19.3N	64.5W
3	07/08/71	05/54/12	194.0	5.0	48	19.1N	68.0W	18N	69W	23.2N	67.1W	19.2N	69.9W	18.5N	68.8W
4	08/27/71	06/37/53	193.1	4.7	33	19.2N	68.1W	18N	69W	23.2N	67.2W	19.2N	69.9W	18.5N	68.7W
5	09/13/71	09/00/26	203.4	4.7	44	6.9N	71.8W	7N	72W	6.4N	72.7W	7.4N	72.2W	7.2N	72.5W
6	09/21/71	20/31/09	208.5	4.8	150	6.8N	73.1W	6N	73W	7.7N	72.5W	6.6N	73.3W	6.3N	73.1W
7	09/30/71	20/27/58	161.2	4.9	152	18.1N	64.5W	17N	65W	20.0N	63.9W	17.7N	65.5W	17.2N	64.7W
8	11/15/71	00/02/09	208.7	4.8	164	6.8N	73.1W	6N	72W	8.6N	71.3W	6.9N	72.4W	7.2N	72.7W
9	11/22/71	04/55/00	202.9	4.8	36	8.8N	71.2W	8N	72W	10.4N	69.1W	6.9N	71.3W	7.4N	71.7W
10	11/25/71	11/12/25	209.7	5.1	159	6.8N	73.0W	6N	73W	8.9N	71.0W	5.9N	72.9W	6.2N	73.2W
11	12/23/71	00/08/50	132.2	4.8	16	14.6N	60.9W	14N	61W	17.8N	58.9W	14.3N	61.1W	14.2N	61.0W
12	12/23/71	13/17/08	135.0	4.7	170	15.1N	61.4W	13N	61W	14.2N	62.4W	14.6N	62.3W	14.2N	61.6W
13	12/30/71	05/00/13	226.7	4.9	43	5.6N	77.7W	6N	74W	6.4N	78.0W	10.0N	76.2W	9.0N	75.4W
14	01/03/72	07/25/23	143.3	5.0	67	10.7N	62.7W	11N	62W	12.7N	60.6W	10.9N	61.8W	11.2N	62.4W
15	01/20/72	16/31/47	239.3	4.5	82	6.7N	75.6W	7N	74W	9.0N	73.6W	7.8N	74.4W	9.8N	76.0W

TABLE 2

The NOAA focal parameters for earthquakes in the Kurile Islands used in analysis (see also Fig 3). The event locations given in the LASA and NORSAR bulletins are included, and also the epicenter solutions based on two-array azimuth and azimuth and arrival time observations. The LASA and NORSAR azimuth values used were computed from the respective one-array locations while arrival time differences are listed in the T_N-T_L column.

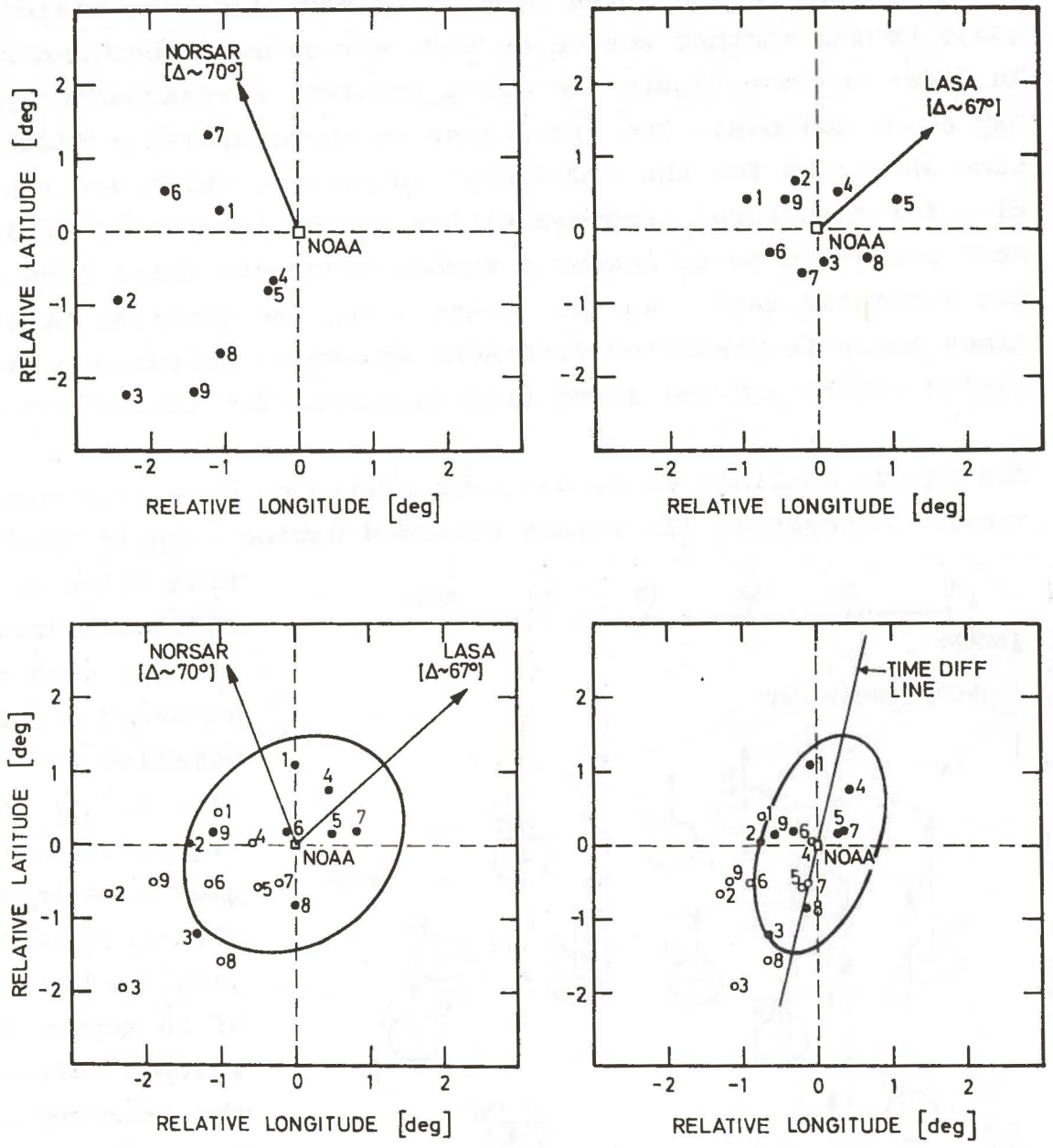

Fig 3. NORSAR and LASA epicenter locations for 9 earthquakes in the Kurile Islands region compared to those of NOAA. A biased error in azimuth of 1.0 deg seems to occur in the NORSAR data. The open and closed rings indicate biased and unbiased observations. The given 95% confidence ellipses are based on standard deviations of 0.5 deg in azimuths and 2.0 sec in arrival times.

BIASED OBSERVATIONAL ERRORS

Heterogeneous structures in the site and source regions may cause systematic delays in the P-wave travel times across an array, and henceforth biased errors in the estimated azimuth and slowness of the incoming wavefronts. From our point of view the most interesting aspect of the above problem is how large the biased errors could be and whether source or site structural anomalies dominate. In order to investigate the above problem, a reasonable approach may be as follows: The first step is to establish a model for time anomalies for the individual subarrays, which are representative for structural inhomogeneities in the array site area. The next one would be to locate a number of events using both observed and simulated data. In the latter case, the subarray arrival times would be predicted from NOAA epicenter solutions, Herrin's tables (1968) and the above time anomalies for the siting area.

The method outlined above has been tested on data from the NORSAR array. Altogether 126 events recorded during interim NORSAR operation (Plan D) Jan-Jun 1970 were analyzed. At this time only 18 subarray center seismometers were operative (see Fig 4) and the high-quality P-signals used were in each case clearly visible on at least 14 out of the total of 18 sensor traces. The station corrections on the subarray level were computed in the ordinary way, i.e., taking the average of the difference between observed and predicted arrival times across the array. The resulting one-dimensional model for the subarray station time delays for NORSAR is shown in Fig 4

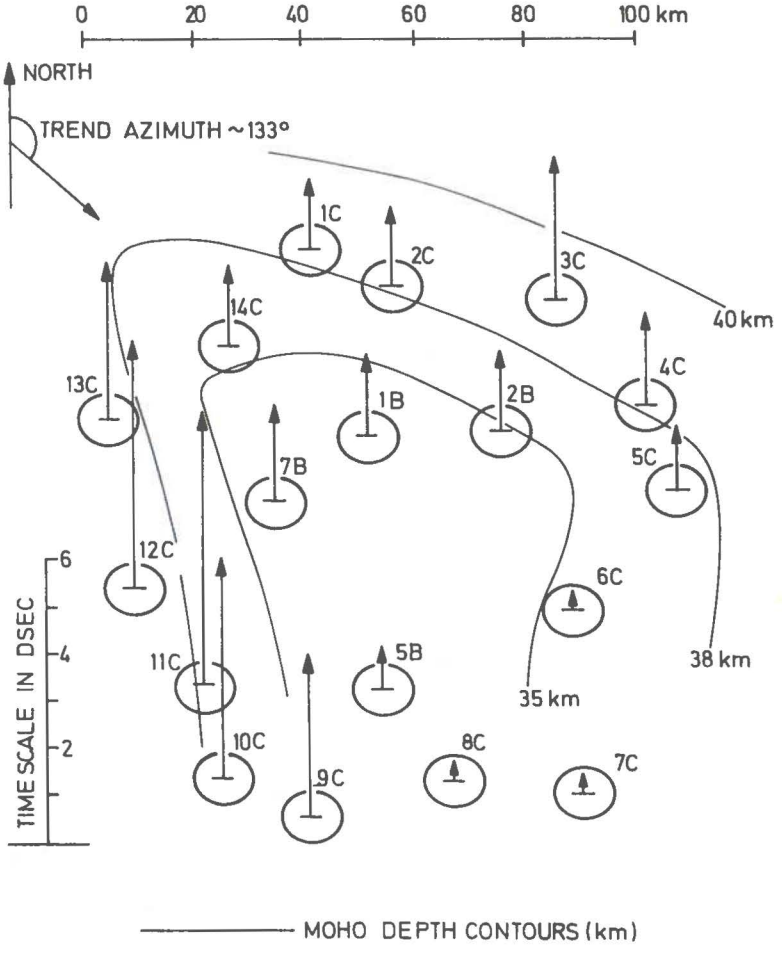

Fig 4. Observed time delays plotted as a function of NORSAR subarray configuration. The MOHO depth contours are taken from a paper by Kanestrøm and Haugland (1971).

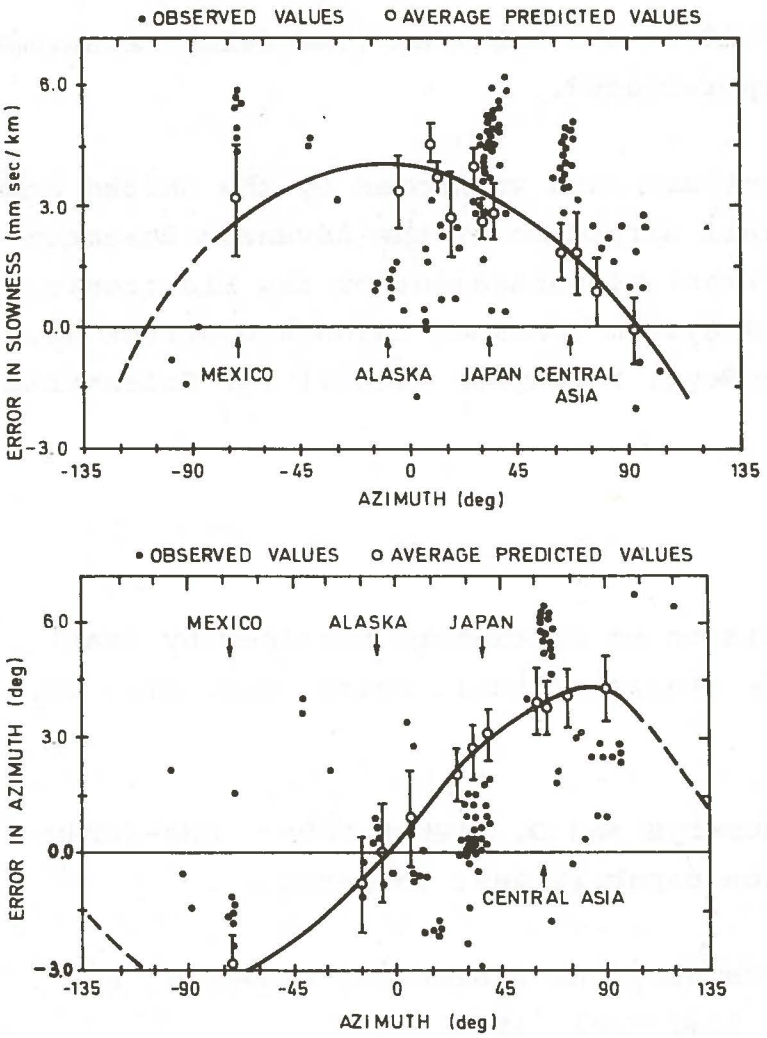

Fig 5. Observed and simulated biased observational errors in slowness and azimuth for the NORSAR array.

and is considered acceptable as a first order approximation for simulating biased location errors. In the latter case, the obtained results are shown in Fig 5 where the mislocation vectors are split into epicentral distance, independent azimuth and velocity bias components. For computational details we again refer to Gjøystdal et al, 1972.

The result presented in Fig 5 exhibits several interesting features. First of all, structural anomalies in the siting area account for roughly about 50 per cent of the bias in observed P-wave azimuth and slowness. Moreover, the absolute value of the mislocation vector and hence its gradient are relatively large especially in view of NORSAR's array diameter of around 110 km. In practice, this means that in order to avoid excessive errors in event locations based on a single array like NORSAR, extensive calibration files are part of its software system. However, for epicentral distances beyond 85 degrees and including most of the core shadow zone, where the gradients of the slowness curves are small, large mislocations are likely to occur, unless secondary arrivals, seismicity or external information are available.

ACKNOWLEDGEMENTS

Mr. K.A. Berteussen assisted in the subarray time delay measurements, and his help is greatly appreciated.

The NORSAR research project has been sponsored by the United States of America under the overall direction of the Advanced Research Projects Agency and the technical management of the Electronic System Division, Air Force System Command, through Contract No. F19628-70-C-0283 with the Royal Norwegian Council for Scientific and Industrial Research.

REFERENCES

1. J.F. Evernden: Precision of epicenters obtained by small numbers of world-wide stations, Bull. Seism. Soc. Am., 59, 1365-1398, 1969.

2. H. Gjøystdal, E.S. Husebye and D. Rieber-Mohn: One-array and two-array location capabilities, In press.

3. E. Herrin et al: Seismological tables for P phases, Bull. Seism. Soc. Am., 58, 1193-1241, 1968.

4. R. Kanestrøm and K. Haugland: Crustal structure in south-eastern Norway from seismic refraction measurements, Sci. Rep. No. 5, Seismological Observatory, Univ. of Bergen, 1971.